Perturbed-TEM Analysis of Transmission Lines with Imperfect Conductors

I-SHENG TSAI, STUDENT MEMBER, IEEE, AND CHUN HSIUNG CHEN, SENIOR MEMBER, IEEE

Abstract—**A novel perturbed-TEM approach is proposed to study the detailed current distribution and the propagation constant of a multiconductor transmission line system with imperfect conductors. In this study, the perturbed fields are derived under the assumption that the fields outside the conductors are TEM waves of the corresponding lossless system and those inside the conductors satisfy the TM modal equations. These fields are then substituted into a perturbational formula to obtain the propagation constant of the lossy system. Presented as an example are the current distribution and the propagation constant of a lossy two-wire transmission line, which clearly illustrates the loss mechanism due to the skin effect and the proximity effect.**

I. Introduction

THE MODELING of conductor loss in a multiconductor transmission line system is again receiving attention due to the advent of high-speed integrated circuits. As the speed goes higher and the circuit size gets smaller, the circuit dimension becomes comparable to the skin depth. Under such a condition, the skin effect and the proximity effect may force the currents to gather toward the surfaces and near sides of the conductors. This modification of the current distribution makes the power loss, and therefore the attenuation constant, frequency dependent.

Although studies of conductor loss started very early, most of them have treated only cases with circuit dimensions much greater than the skin depth [1]–[5]. The power loss was then obtained by the surface resistance method [1]–[4] once the current distribution of the related lossless system could be calculated in advance, or by the incremental induction rule [5] if the inductance of the lossless system could be found analytically. The common assumption in these methods is the exponentially decaying behavior of the current distributions.

It is not until recently that detailed current distributions have been given serious attention. Waldow and Wolff [6] used a variational formulation for studying the skin effect problem. For the same skin effect problem, Konrad [7], [8] and Costache [9] developed an integrodifferential finite element approach. To carry out the numerical computation, both methods [6]–[9] have to assume an artificial boundary box to confine the problem in a finite region. Alternatively, Weeks *et al.* [10] have proposed a volume integral equation method based on network theory. In the high-frequency range, all the above methods are faced with a large matrix problem, which may require a great deal of time in numerical calculation. Djordjevic *et al.* [11] applied the surface integral equation approach, which was numerically efficient for most of the frequencies. However, an additional unnecessary radiation resistance would appear at higher frequency due to the axial-independent TM wave assumption. Recently, Wu and Yang [12] successfully proposed a similar surface integral equation approach to tackle the skin effect problem where an axial and sinusoidal quasi-TEM modal field was assumed.

In this paper, a perturbational formulation of the propagation constant [13] is proposed to study the skin effect and proximity effect of a multiconductor transmission line system. By assuming that the fields outside the conductors are TEM waves of the corresponding lossless system and that those inside satisfy the modified equations of TM modal fields, suitable perturbed TEM fields may be derived for calculating the propagation constant from the perturbational formula. The numerical results of a lossy two-wire transmission line are presented as a demonstration of this approach, and they illustrate clearly the skin effect and the proximity effect.

II. Perturbational Formulation of the Propagation Constant

Consider a lossy transmission line system (the perturbed system) of N imperfect electric conductors, $\Omega_i(\mu_i, \epsilon_i, \sigma_i;\ i = 1, 2, \cdots, N)$, in a lossless region $\Omega(\mu_0, \epsilon_0)$ as shown in Fig. 1. Each conductor has conductivity σ_i, permeability μ_i, and permittivity ϵ_i, respectively. By perturbational technique, one needs the related lossless system (the unperturbed system) in which the conductors in Fig. 1 are replaced by perfect electric conductors of the same shapes. Conventionally, the attenuation constant α of the lossy system is calculated by the power-loss formula [1]

$$\alpha = \frac{P_L}{2P} \tag{1}$$

Manuscript received August 14, 1989; revised January 30, 1990. This work was supported by the National Science Council, Republic of China, under Grant NSC 79-0404-E002-39.

The authors are with the Department of Electrical Engineering, National Taiwan University, Taipei 10764, Taiwan, Republic of China.

IEEE Log Number 9034889.

0018-9480/90/0600-0754$01.00 ©1990 IEEE

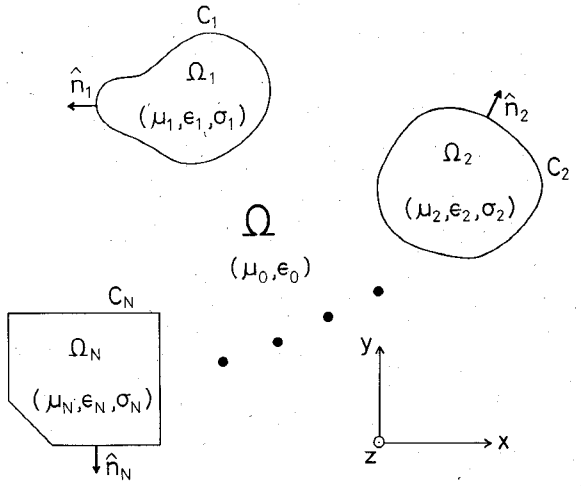

Fig. 1. Geometry of lossy multiconductor transmission line system.

where P_L is the power loss per unit length and P is the power flow along the line. In this study, the perturbational formula [13]

$$\gamma - \gamma_0 = \frac{\sum_{i=1}^{N} \oint_{C_i} (\hat{n}_i \times \boldsymbol{E}) \cdot \boldsymbol{H}_0 \, dl}{\iint_{\Omega} (\boldsymbol{E} \times \boldsymbol{H}_0 - \boldsymbol{E}_0 \times \boldsymbol{H}) \cdot \hat{z} \, dx \, dy} \tag{2}$$

will be adopted to characterize the propagation constant γ of the lossy system. Here $(\boldsymbol{E}, \boldsymbol{H})$ are the fields of the lossy system (Fig. 1) propagating in the negative z direction with $\gamma = \alpha + j\beta$. $(\boldsymbol{E}_0, \boldsymbol{H}_0)$ are the fields of the related lossless system propagating in the positive z direction with the propagation constant $\gamma_0 = j\beta_0$. Also, $\hat{n}_i$ represents the unit normal vector pointing outward from the surface contour C_i of each conductor, and Ω is the region outside the conductors. Note that formula (2) includes the change of the wavenumber $\beta - \beta_0$ while formula (1) does not.

It should be mentioned that both formulas (1) and (2) are exact if exact fields for $(\boldsymbol{E}, \boldsymbol{H})$ are substituted into these formulas. Using the perturbational formulation, a suitable approximation is used for the $(\boldsymbol{E}, \boldsymbol{H})$ fields instead of the exact ones. For instance, the unperturbed fields $(\boldsymbol{E}_0, \boldsymbol{H}_0)$ may be utilized to compute the powers P_L and P in formula (1). Alternative approximate fields are obtained based on the assumptions that the fields of the lossy system outside the conductors would be almost the same as those of the lossless system, and that the electric currents inside the conductors would exhibit an exponentially decaying behavior. Under such assumptions, both (1) and (2) would predict the same result:

$$\alpha = \mathrm{Re}[\gamma - \gamma_0] = \frac{\sum_{i=1}^{N} R_{si} \oint_{C_i} |\boldsymbol{H}_0|^2 \, dl}{2 \iint_{\Omega} \mathrm{Re}[\boldsymbol{E}_0 \times \boldsymbol{H}_0^*] \cdot \hat{z} \, dx \, dy} \tag{3}$$

where $R_{si} = (\pi f \mu_i / \sigma_i)^{1/2}$ is the surface resistance and f is the operating frequency.

Very often the exponentially decaying assumption is not satisfied, especially when the skin depth is no longer much smaller than the dimensions of the conductors. Then one may use the approximate fields derived from the quasi-TEM modal analysis [12]. The main assumptions of this analysis are that the fields outside the conductors are TEM waves in nature and the fields inside the conductors are TM fields with $\boldsymbol{E} \simeq \hat{z} E_z$. Under such assumptions, the approximate fields (with the factor $\exp[j(\omega t + \beta_0 z)]$ omitted) may be expressed as

$$\begin{cases} \boldsymbol{H} = \nabla_t \varphi \times \hat{z} / \mu_i \\ \boldsymbol{E} = \hat{z} \nabla_t^2 \varphi / \mu_i \sigma_i \end{cases} \quad \text{for } (x, y) \text{ in } \Omega_i \tag{4a}$$

$$\begin{cases} \boldsymbol{H} = \nabla_t \varphi \times \hat{z} / \mu_0 \\ \boldsymbol{E} = \nabla_t \varphi / \sqrt{\mu_0 \epsilon_0} \end{cases} \quad \text{for } (x, y) \text{ in } \Omega \tag{4b}$$

where the potential function φ satisfies

$$(\nabla_t^2 - j\omega \mu_i \sigma_i) \varphi(x, y) = -\sigma_i V_i \quad \text{for } (x, y) \text{ in } \Omega_i \tag{5a}$$

$$\nabla_t^2 \varphi(x, y) = 0 \quad \text{for } (x, y) \text{ in } \Omega. \tag{5b}$$

Here $\nabla_t = \hat{x} \partial / \partial x + \hat{y} \partial / \partial y$, $\nabla_t^2 = \partial^2 / \partial x^2 + \partial^2 / \partial y^2$, and V_i (a constant inside each conductor) is the voltage drop per unit length. Equation (5) together with the conditions that φ and the tangential magnetic field are continuous across the conductor boundaries can be used to solve the perturbed EM fields.

The approximate fields (4) and (5) were used in [12] to obtain the equivalent circuit parameters of the line such as resistance R and inductance L. In this study, their modifications, (6), will be substituted into formula (2) to obtain the propagation constant of the same line. Note that outside the conductors $\boldsymbol{H}$ is approximately equal to $-\boldsymbol{H}_0^*$ and $(\boldsymbol{E}, \boldsymbol{H})$ depend only on the derivatives of φ. So one may add any constant to φ without changing the field distribution. By this argument, one has the modified equations

$$(\nabla_t^2 - j\omega \mu_i \sigma_i) \varphi(x, y) = 0 \quad \text{for } (x, y) \text{ in } \Omega_i \tag{6a}$$

$$\hat{n}_i \cdot (\mu_i^{-1} \nabla_t \varphi - \boldsymbol{H}_0^* \times \hat{z}) = 0 \quad \text{for } (x, y) \text{ on } C_i \tag{6b}$$

for the perturbed EM fields $(\boldsymbol{E}, \boldsymbol{H})$ employed in (2).

III. Two-Wire Transmission Line with Imperfect Conductors

To demonstrate the application of the perturbational formula (2), let us consider the lossy two-wire transmission line system (Fig. 2) which consists of two round wires $(\mu_0, \epsilon_0, \sigma)$ of radii a_1 and a_2 with a distance D between the wire centers. Its unperturbed fields may be expressed as

$$\boldsymbol{H}_0 = \mu_0^{-1} \nabla_t \varphi_0 \times \hat{z} \tag{7a}$$

$$\boldsymbol{E}_0 = -\nabla_t \varphi_0 / \sqrt{\mu_0 \epsilon_0} \tag{7b}$$

where the scalar potential φ_0 for the lossless system is

$$\varphi_0 = \mu_0 I_0 \ln \left[\frac{(x - D_1 - b)^2 + y^2}{(x - D_1 + b)^2 + y^2} \right]^{1/2}. \tag{8}$$

Here $D_1 = (D^2 + a_1^2 - a_2^2)/2D$, $b = (D_1^2 - a_1^2)^{1/2}$, and I_0 is the total current along the wire.

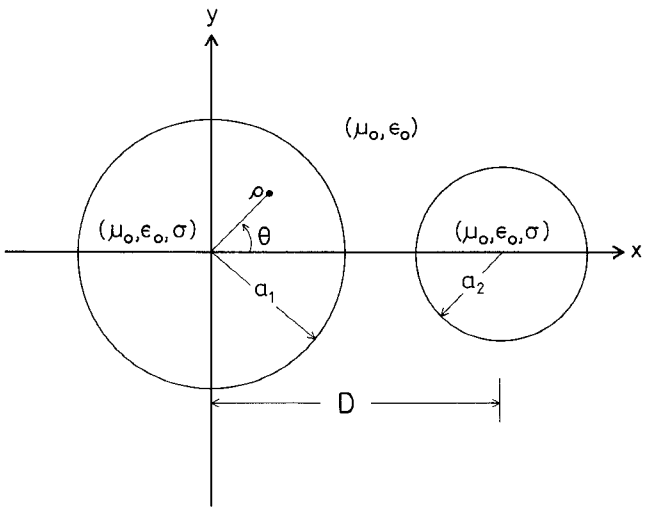

Fig. 2. Geometry of lossy two-wire transmission line system.

The next step is to find the perturbed fields $(\boldsymbol{E}, \boldsymbol{H})$, (4), inside the conductors. By using (6) and adopting polar coordinates (ρ, θ), the potential inside the left conductor can be written as

$$\varphi = \sum_{m=0}^{\infty} \varphi_m J_m(k\rho) \cos m\theta \tag{9a}$$

$$\varphi_m = \frac{-I_0\mu_0}{\pi k a_1 \epsilon_m J_m'(ka_1)} \left(e_1 - \sqrt{e_1^2 - 1}\right)^m. \tag{9b}$$

Here $k^2 = -j\omega\mu_0\sigma$, $J_m(k\rho)$ is Bessel's function of order m with complex argument $k\rho$; $e_1 = D_1/a_1$; and $\epsilon_m = 2$ $(m = 0)$ or 1 $(m \geqslant 1)$. A similar expression for the potential inside the right conductor can also be derived. By using the perturbed and unperturbed fields, (9) and (8), the propagation constant in (2) then reduces to

$$\gamma - \gamma_0 = \frac{j\omega}{ck\left(\cosh^{-1}e_1 + \cosh^{-1}e_2\right)} \times \sum_{i=1}^{2} \sum_{m=0}^{\infty} \frac{J_m(ka_i)}{a_i \epsilon_m J_m'(ka_i)} \left(e_i - \sqrt{e_i^2 - 1}\right)^{2m} \tag{10}$$

where $e_i = D_i/a_i$, $D_2 = D - D_1$, and c is the speed of light in free space. The current density $J_z (= \sigma E_z = j\omega\sigma\varphi)$ in the left conductor can be written as

$$J_z = -j\omega\sigma \sum_{m=0}^{\infty} \frac{I_0\mu_0 J_m(k\rho)\cos m\theta}{\pi k a_1 \epsilon_m J_m'(ka_1)} \left(e_1 - \sqrt{e_1^2 - 1}\right)^m. \tag{11}$$

The expressions for large or small $|ka_i|$ are worth special consideration. When $|ka_i|$ are much greater than unity, which is equivalent to the case where a_i are greater than the skin depth, $J_m'(ka_i)$ are approximately equal to $jJ_m(ka_i)$ so the infinite series of (10) can be analytically calculated:

$$\gamma - \gamma_0 = \frac{(1+j)\sqrt{\omega\epsilon_0/2\sigma}}{2\left(\cosh^{-1}e_1 + \cosh^{-1}e_2\right)} \sum_{i=1}^{2} \frac{e_i}{a_i\sqrt{e_i^2 - 1}}. \tag{12}$$

This same result for $a_1 = a_2$ has been presented in [1]. Equation (12) also shows that the attenuation constant α is proportional to the square root of the frequency. This is the well-known result at higher frequency. In the lower frequency range where $|ka_i|$ are much less than unity so that $J_0(ka_i) \simeq 1$, $J_1(ka_i) \simeq ka_i/2$, and $J_m(ka_i) \simeq 0$ for $m \geqslant 2$, equation (10) can be simplified to

$$\gamma - \gamma_0 = \frac{a_1^{-2} + a_2^{-2}}{c\mu_0\sigma\left(\cosh^{-1}e_1 + \cosh^{-1}e_2\right)} + O(\omega). \tag{13}$$

Thus the attenuation constant approaches a certain constant as the frequency approaches zero. Such a result is expected because the current distribution becomes uniform as the radii become smaller than the skin depth.

A scaling relation in (11) is observed if the current density J_z is normalized by the uniform one: $J_0 = I_0/\pi a_1^2$. By keeping ka_1 constant, the normalized current J_z/J_0 will remain unchanged when the wire geometry is enlarged and the frequency is reduced properly.

IV. Numerical Results

A computer program based on (10) and (11) is established to calculate the propagation constant and the current distribution of the two-wire transmission line system (Fig. 2). The infinite series in these equations converge rapidly because the term $(e_i - \sqrt{e_i^2 - 1})$ is less than unity. This term is approximately proportional to $(2e_i)^{-1}$; thus the larger the ratio $e_i = D_i/a_i$ the more rapid the convergence. On a VAX 8700, the computer program takes only 0.25 s in calculating 20 data points of the attenuation constant. In Wu's approach [12], where the surface integral equation method is used and the circular contour is approximated by a regular polygon of 16 edges, computation of the same data points would take more than 4 min on a VAX 8700.

In the following discussion, we present only the amplitude of the dimensionless current distribution $|J_z|$, which is normalized by the uniform current density $J_0 = I_0/\pi a_1^2$. The assumed conductivity σ is 5.7×10^7 S/m.

To examine the validity of the theory and the accuracy of the program, the current distributions of the present approach are compared with those of [12] and [14] in Fig. 3. Carson's results are reproduced from formulas (15) and (42) of [14], after using the approximations (40) and (41) of [14], to get the closed-form coefficients of the series solution for the current distribution. Good agreement between the results for $D/a = 5$ and 500 is observed and those of [12] and [14] are not shown. For the case $D/a = 2.5$, where the two wires are very close, the results of [14] are quite different from those of [12] and ours, while the latter two show only slight difference. For small D/a the approximations in (40) and (41) of [14] are inadequate. To obtain better results, the complicated infinite-dimensional matrix equation [14, eq. (34)] has to be solved for the coefficients of the current series. Then the advantage of the analytic approach in [14] will disappear and the procedure will become more like the numerical method used in [12].

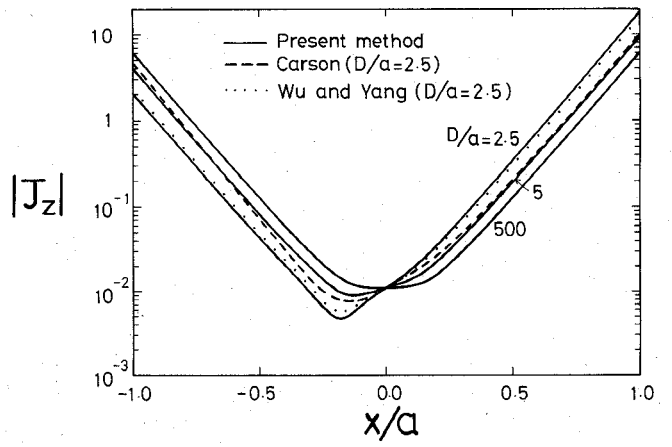

Fig. 3. Normalized current distributions $|J_z|$ with D/a as parameters: $a_1 = a_2 = a = 4$ cm, $\sigma = 5.7\times10^7$ S/m, and $f = 200$ Hz. The results of [12] and [14] are also shown for comparison. All current densities are normalized by the uniform one: $J_0 = I_0/\pi a_1^2$.

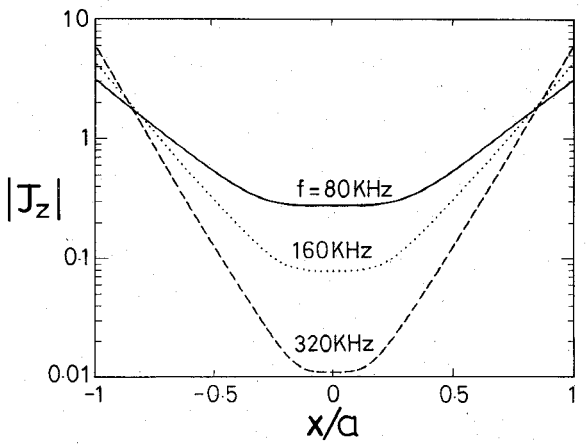

Fig. 4. Current distributions to show skin effect at higher frequencies: $a_1 = a_2 = a = 1$ mm, $D/a = 500$, and $\sigma = 5.7\times10^7$ S/m.

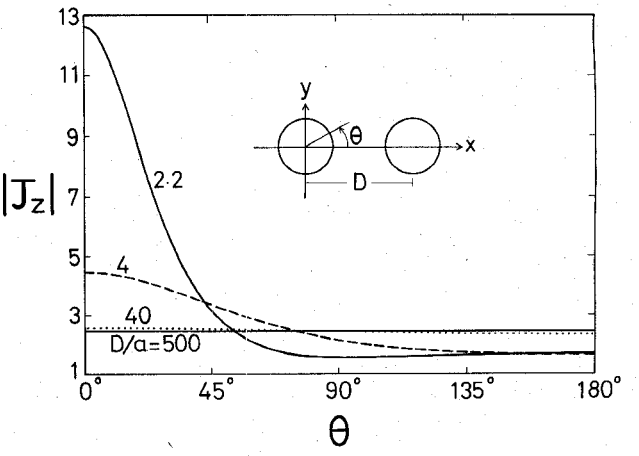

Fig. 5. Currents on left-conductor surface to reflect proximity effect: $a_1 = a_2 = a = 1$ mm, $\sigma = 5.7\times10^7$ S/m, and $f = 10$ kHz.

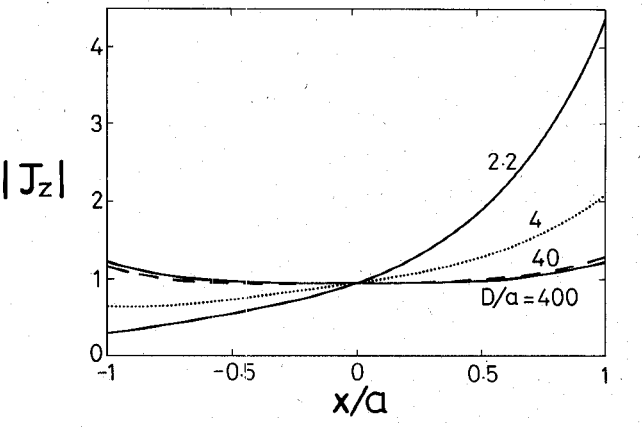

Fig. 6. Currents to show proximity effect by adjusting D/a: $a_1 = a_2 = a = 1$ mm, $\sigma = 5.7\times10^7$ S/m, and $f = 10$ kHz.

The current distributions in Figs. 3 and 4 are plotted on logarithmic scales to show the exponentially decaying phenomenon at high frequency. The slopes of the curves at the conductor surfaces reflect the frequency dependence of the skin depth. Because frequency is kept constant in Fig. 3, the slopes of the curves are the same. But as the distance D between wire centers gets smaller, the normalized current density at the near end $x = a_1$ becomes much larger than that at the far end $x = -a_1$. This is due to the proximity effect.

Shown in Fig. 4 are the current distributions when the distance between the two wires is large so that the skin effect is much larger than the proximity effect. By the scaling argument, our normalized currents at $f = 0.08$, 0.16, and 0.32 MHz should be the same as those of [12] at $f = 50$, 100, and 200 Hz. In fact, the results of [12] and our results are well matched; therefore only ours are plotted. In addition, the slopes of these curves are proportional to the square root of the frequency, which in turn is proportional to the inverse of the skin depth.

The variation of the current density on the left-conductor surface is plotted in Fig. 5. It should be noticed that the order of magnitude does not vary much, and that the current density at the conductor surface is governed by the proximity effect alone. The proximity effect is negligible, as reflected by the constant surface current, when the distance D is sufficiently large. The proximity effect makes $|J_z|$ larger at the near end ($\theta = 0$) as D is decreased.

To highlight the proximity effect, a lower frequency case is chosen so that the skin effect is less significant. In Figs. 6 and 7, the exponentially decaying phenomenon due to skin effect disappears and the variation in current comes from the proximity effect. With large D/a the current distribution is almost uniform, while with small D/a it increases monotonically from the far end to the near end, as shown in Fig. 6. The influence of the right-wire size on the left-wire current is shown in Fig. 7. When the ratio a_2/a_1 is small, $|J_z|$ shows little dependence on the wire radius a_2. But as a_2/a_1 becomes large, the proximity effect can greatly affect the current distribution $|J_z|$ in the left wire.

Redistribution of current density due to skin and proximity effects causes the propagation constant to change accordingly. Fig. 8 shows the dependence of the attenuation constant α on frequency. It can be seen that α is proportional to the square root of frequency in the high-

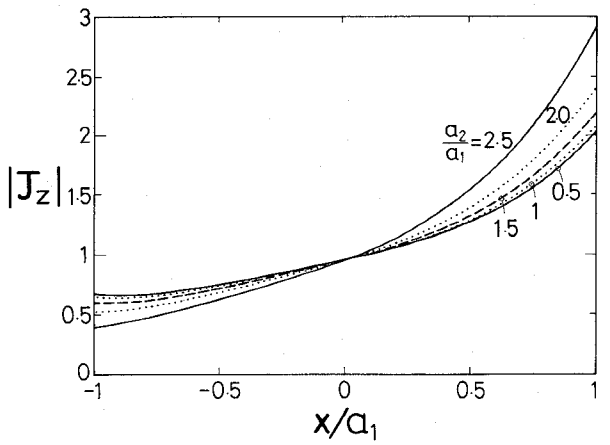

Fig. 7. Currents to show proximity effect by varying a_2/a_1: $a_1 = 1$ mm, $D/a_1 = 4$, $\sigma = 5.7\times10^7$ S/m, and $f = 10$ kHz.

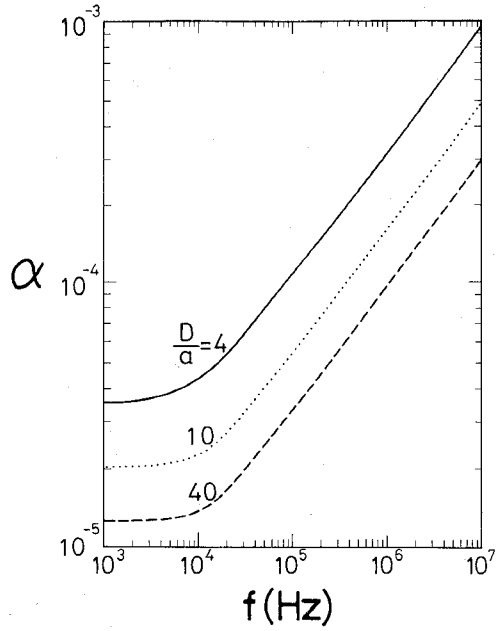

Fig. 8. Attenuation constant α (Np/m) versus frequency f (Hz) with D/a as parameters: $a_1 = a_2 = a = 1$ mm and $\sigma = 5.7\times10^7$ S/m.

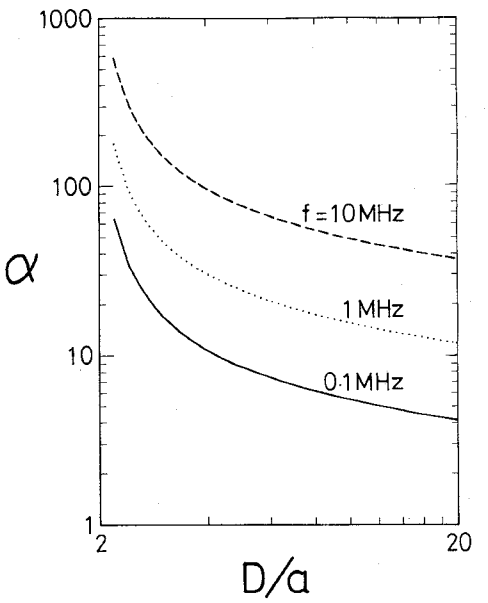

Fig. 9. Attenuation constant α versus D/a with frequency f as parameters: $a_1 = a_2 = a = 1$ mm and $\sigma = 5.7\times10^7$ S/m.

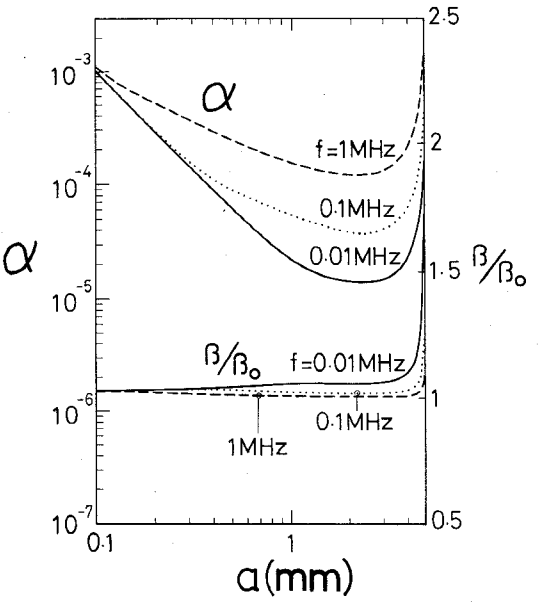

Fig. 10. Attenuation constant α and normalized wavenumber β/β_0 versus wire radius a $(= a_1 = a_2)$ with frequency f as parameter. $D = 10$ mm and $\sigma = 5.7\times10^7$ S/m.

frequency range and tends to a constant in the low-frequency range. The attenuation constant increases as the wire distance D is decreased due to the proximity effect, as illustrated in Fig. 9. The variation of α decreases as D becomes large because the two wires now act almost independently when they are far apart. The effect of wire radius a on the attenuation constant α and the normalized wavenumber β/β_0 is shown in Fig. 10. For thin wires, the current distribution is essentially uniform so that α is inversely proportional to the square of a. For large a such that the two wires almost touch, both α and β/β_0 tend to infinity. The assumption that β should be approximately equal to β_0 is no longer satisfied; thus the validity of the theory is questionable when the two wires are too close together. The effect of varying a_2/a_1 on the attenuation constant is shown in Fig. 11. When a_2/a_1 is small and frequency is low, increasing a_2/a_1 will lower α because the larger right wire has reduced the power loss. But when a_2/a_1 is large and the proximity effect is dominant, α will increase as a_2/a_1 is further increased.

V. Conclusions

The current distribution and the propagation constant of a two-wire transmission line system have been studied using the perturbed-TEM approach. The wave behavior due to the skin effect and the proximity effect has been clearly displayed. Being simple in structure, many calculations can be done analytically and the actual CPU time can be considerably reduced. In a more general structure such analytical convenience may disappear. However, the

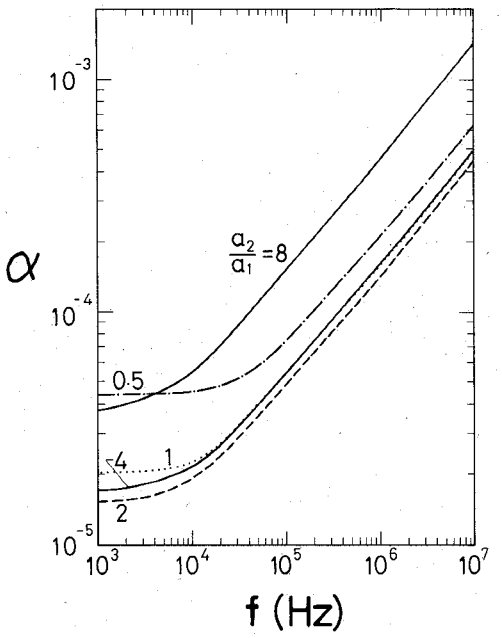

Fig. 11. Attenuation constant α versus f with a_2/a_1 as parameters: $a_1 = 1$ mm, $D/a_1 = 10$ and $\sigma = 5.7\times10^7$ S/m.

same perturbed-TEM analysis is still applicable. A possible extension of this method to deal with the multiconductor system with imperfect conductors in an inhomogeneous medium, such as the microstrip line, is under consideration. By treating the transverse magnetic field component of the corresponding lossless system as the boundary condition, the same technique then leads to the desired propagation constant.

Acknowledgment

The authors would like to express their appreciation to Prof. R. B. Wu, J. C. Yang, and the reviewers for many valuable discussions and comments.

References

[1] R. E. Collin, *Field Theory of Guided Waves*. New York: McGraw-Hill, 1960. pp. 126–127 and p. 166.

[2] B. E. Spielman, "Dissipative loss effects in isolated and coupled transmission lines," *IEEE Trans. Microwave Theory Tech.*, vol. MTT-25, pp. 648–656, Aug. 1977.

[3] R. H. Jansen, "High-speed computation of single and coupled microstrip parameters including dispersion, high-order modes, loss and finite strip thickness," *IEEE Trans. Microwave Theory Tech.*, vol. MTT-26, pp. 75–82, Feb. 1978.

[4] D. Mirshekar-Syahkal and J. B. Davies, "Accurate solution of microstrip and coplanar structures for dispersion and for dielectric and conductor losses," *IEEE Trans. Microwave Theory Tech.*, vol. MTT-27, pp. 694–699, July 1979.

[5] R. A. Pucel, D. J. Masse, and C. P. Hartwig, "Losses in microstrip," *IEEE Trans. Microwave Theory Tech.*, vol. MTT-16, pp. 342–350, June 1968.

[6] P. Waldow and I. Wolff, "The skin-effect at high frequencies," *IEEE Trans. Microwave Theory Tech.*, vol. MTT-33, pp. 1076–1082, Oct. 1985.

[7] A. Konrad, "The numerical solution of steady-state skin effect problems—An integrodifferential approach," *IEEE Trans. Magn.*, vol. MAG-17, pp. 1148–1152, Jan. 1981.

[8] A. Konrad, "Integrodifferential finite element formulation of two-dimensional steady-state skin effect problems," *IEEE Trans. Magn.*, vol. MAG-18, pp. 284–292, Jan. 1982.

[9] G. I. Costache, "Finite element method applied to skin-effect problems in strip transmission lines," *IEEE Trans. Microwave Theory Tech.*, vol. MTT-35, pp. 1009–1013, Nov. 1987.

[10] W. T. Weeks, L. L. Wu, M. F. McAllister, and A. Singh, "Resistive and inductive skin effect in rectangular conductors," *IBM. J. Res. Develop.*, vol. 23, pp. 652–660, Nov. 1979.

[11] A. R. Djordjevic, T. K. Sarkar, and S. M. Rao, "Analysis of finite conductivity cylindrical conductors excited by axially-independent TM electromagnetic field," *IEEE Trans. Microwave Theory Tech.*, vol. MTT-33, pp. 960–966, Oct. 1985.

[12] R. B. Wu and J. C. Yang, "Boundary integral equation formulation of skin effect problems in multiconductor transmission lines," *IEEE Trans. Magn.*, vol. MAG-25, pp. 3013–3015, July 1989.

[13] R. F. Harrington, *Time-Harmonic Electromagnetic Fields*. New York: McGraw-Hill, 1961, p. 375.

[14] J. R. Carson, "Wave propagation over parallel wires: The proximity effect," *Phil. Mag.*, S. 6., vol. 41, no. 24, pp. 607–633, Apr. 1921.

I-Sheng Tsai (S'89) was born in Kaohsiung, Taiwan, Republic of China, on March 6, 1963. He received the B.S.E.E. degree in June 1984 from National Taiwan University, Taipei, Taiwan. Since 1984 he has been working toward the Ph.D. degree at the same university. His current topics of interest include the analysis of microwave and millimeter-wave integrated circuits, field theory, and numerical techniques in electromagnetics.

Chun Hsiung Chen (SM'88) was born in Taipei, Taiwan, Republic of China, on March 7, 1937. He received the B.S.E.E. degree from National Taiwan University, Taipei, Taiwan, in 1960, the M.S.E.E. degree from National Chiao Tung University, Hsinchu, Taiwan, in 1962, and the Ph.D. degree in electrical engineering from National Taiwan University in 1972.

In 1963, he joined the faculty of the Department of Electrical Engineering, National Taiwan University, where he is now a Professor. From August 1982 to July 1985 he was Chairman of the department. In 1974 he was a Visiting Researcher for one year in the Department of Electrical Engineering and Computer Sciences, University of California, Berkeley. From August 1986 to July 1987, he was a Visiting Professor in the Department of Electrical Engineering, University of Houston, Texas. In June and July 1989 he visited the Microwave Department, Technical University of Munich, West Germany. His areas of interest include antenna and waveguide analysis, propagation and scattering of waves, and numerical techniques in electromagnetics.